Table 3. Conventional radiocarbon ages, with 1 $\sigma$ statistical counting errors (*12*) and most probable historical ages of charcoal samples from Anza, Yugoslavia, derived in the same manner as for the samples listed in Table 2.

| Archeological stratum | Field number | Laboratory number | Conventional radiocarbon age (years B.P.) | | | | Most probable historical date (years B.C.) |
|---|---|---|---|---|---|---|---|
| | | | La Jolla | | | | |
| | | | M & B counters | Tim counters or one counter | UCLA | Average | |
| IV | VIII 55 | 2411 | | 6070 ± 190 | | | |
| | XX 190 | 2329 | 6210 ± 60 | | | 6200 ± 60 | 5200 |
| III | V 62 | 2185 | | 6510 ± 110 | | | |
| | L 19 | 1705B | | | 6540 ± 120 | | |
| | VII 191 | 2345 | | 6540 ± 120 | | | |
| | L 20 | 1705C | | | 6700 ± 80 | 6600 ± 50 | 5500 |
| II | VII 117 | 2344 | | 7000 ± 270 | | | |
| | VII 121 | 2343 | | 7000 ± 280 | | | |
| | VII 177 | 2338 | | 6800 ± 140 | | | |
| | VII 122 | 2337 | | 7080 ± 60 | | | |
| | VII 213,215 | 2405 | | 6940 ± 80 | | | |
| | VII 124 | 2351 | | 7040 ± 90 | | | |
| | VII 156 | 2409 | 6850 ± 50 | | | 6900 ± 35 | |
| Ib | VII 251 | 2342 | | 7100 ± 80 | | | |
| | VII 240 | 2339 | | 7110 ± 80 | | | |
| | VII 253 | 2333 | | 6840 ± 120 | | | |
| | VII 188 | 2341 | | 7230 ± 170 | | | |
| | VII 256 | 2332 | | 7110 ± 120 | | 7100 ± 40 | 6000 |
| Ia | V 90–110 | 3183 | 7150 ± 50 | | | | |
| | V 76–86 | 3186 | 7140 ± 70 | | | | |
| | V 103–120 | 3032 | 7210 ± 50 | | | | |
| | VII 257 | 233011 | 7170 ± 60 | | | | |
| | V 111 | 2181 | | 7270 ± 140 | | 7190 ± 30 | 6100 |

dioxide did not change noticeably between 6400 and 5800 B.C., the absolute historical dates listed in the last column in Table 2 are obtained. It appears that the earliest stratum (Ia) dates from the 65th century B.C. Unfortunately, no datable material from this stratum was available for measurements at La Jolla, but the four determinations [two from the Pennsylvania (*10*) and two from the UCLA (*11*) laboratories] indicate that it is close to 200 years older than the next stage (Ib), which is dated by direct comparison with bristlecone pine wood.

The next younger stages follow in unusually rapid succession, differing in age by hardly more than the counting errors. This could be due to rapid development, or to a drop in $\Delta^{14}C$ during this period. Such a drop would let the older samples appear too young by up to 200 years relative to the younger ones. Therefore, the possibility cannot be entirely excluded that the earliest stages of Achilleion could date from the 66th or even 67th century B.C. Nothing final, however, can be said as long as no wood from this period that has been dated by tree rings is available for $^{14}C$ determinations.

The upper strata of the archeological sequence of Achilleion have ages close to those of the bristlecone pine samples, and therefore $\Delta^{14}C$ changes cannot affect the results. The four stages of period three, IIIa1, IIIa2, IIIb, and IIIc almost certainly belong to the 61st and 60th centuries B.C.

The earliest dates from the Anza settlement (Table 3) are synchronous with the end of Achilleion II or the beginning of Achilleion III. As the cultural and physical characteristics of Anza are closely related to those of Achilleion, it can be deduced that a lapse of about 300 years took place as the Thessalian culture spread northward into the central Balkans. The 12 radiocarbon dates from Anza position its four major periods within a chronology of almost 1000 years. In this way, stratigraphic data combined with radiocarbon dates provide an indispensable yardstick for determining the chronology of the inland portion of the Balkan Peninsula—the formation and duration of the Starčevo and Early Vinča cultures.

C. WESLEY FERGUSON
*Laboratory for Tree-Ring Research, University of Arizona, Tucson 85721*
MARIJA GIMBUTAS
*Institute for Archaeology, University of California, Los Angeles 90024*
HANS E. SUESS
*Department of Chemistry, University of California, San Diego, La Jolla 92093*

### References and Notes

1. C. Tsountas, *Ai oroistorikai akropoleis Diminou neai Sesklo* (Athens, Greece, 1908); A. J. B. Wace and M. S. Thompson, *Prehistoric Thessaly* (Cambridge Univ. Press, Cambridge, England, 1912).
2. V. Milojčič, J. Boessneck, M. Hopf, *Die Deutschen Ausgrabungen auf der Argissa Magula in Thessalien: Beiträge zur ur-und frühgeschichtlichen Archäologie des Mittelmeer-Kulturraumes* (Habelt, Bonn, 1962); J. Milojčič von Zumbusch and V. Milojčič, *Die Deutschen Ausgrabungen auf der Otzaki-Magula in Thessalien 1. Das frühe Neolithikum: Beiträge zur ur-und frühgeschichtlichen Archäologie des Mittelmeer-Kulturraumes* (Habelt, Bonn, 1971).
3. S. Weinberg, *Hesperia* **31**, 158 (1962); R. J. Rodden, *Sci. Am.* **212**, 82 (April 1965); T. W. Jacobsen, *Hesperia* **42**, 45 (1973).
4. M. Gimbutas, *J. Field Archaeol.* **1**, 277 (1974).
5. ———, *ibid*, p. 26.
6. C. W. Ferguson, *Science* **159**, 839 (1968); *Tree-Ring Bull.* **29**, 3 (1969); in *Radiocarbon Variations and Absolute Chronology*, I. U. Olsson, Ed. (Wiley, New York, 1970), p. 237; in *Proceedings of the Eighth International Radiocarbon Dating Conference*, T. A. Rafter and T. Grant-Taylor, Eds. (Lower Hutt, New Zealand, 1972), vol. 1, p. 18; P. E. Damon, *et al.*, *Am. Antiq.* **39**, 350 (1974).
7. H. Becker, private communication.
8. W. F. Cain and H. E. Suess, *J. Geophys. Res.*, in press.
9. C. W. Ferguson, B. Huber, H. E. Suess, *Z. Naturforsch. Teil A* **21**, 1173 (1966); H. E. Suess and C. Strahm, *Antiquity* **44**, 91 (1970).
10. B. Lawn, *Radiocarbon* **17**, 200 (1975).
11. R. Berger and W. F. Libby, *ibid.*, in press.
12. Conventional radiocarbon ages, or "Libby ages," are by definition calculated with a radiocarbon half-life of 5568 years and normalized to a zero age in A.D. 1950. The definition of statistical counting error can be found in most textbooks on statistics or radioactivity.
13. Thanks are due to T. Linick for supervising and to C. Hutto for carrying out the technical operations of radiocarbon determinations. These determinations were financed by NSF grant DES74-22864. Archeological fieldwork was supported by NSF grant Soc. Sci. 73-09168 and dendrochronological research by NSF grant GP-4892.

17 November 1975; revised 5 January 1976

## X-ray Microscopy of Biological Objects with Carbon K$\alpha$ and with Synchrotron Radiation

Abstract. *X-ray micrographs of biological objects have been obtained with a resolution better than 1000 angstroms by using poly(methyl methacrylate) x-ray resist and carbon K$\alpha$ or synchrotron radiation. Synchrotron radiation allows short exposure times; storage rings especially designed as radiation sources and improved x-ray resists would make exposure times under 1 second possible.*

The last few years have seen considerable effort in lithography to fabricate devices of smaller and smaller dimensions. Scanning electron beam systems (*1*) can generate patterns with line widths of less than 0.1 $\mu$m. X-ray lithography (*2–4*) promises a cheap replication technique for such high-resolution patterns. The well-

known technique of x-ray micrography (*5*) is closely related to x-ray lithography, but instead of a mask produced by an electron beam, the specimen to be investigated is brought in proximity to an x-ray resist, and the resulting x-ray copy of the absorption profile in resist is subsequently viewed with a scanning electron beam system (Fig. 1). The recent advances in x-ray lithography make considerable improvements in the quality of x-ray micrographs possible. Electron synchrotrons or storage rings (*6, 7*) seem to be ideal sources for x-ray lithography and micrography. They have a higher intensity of soft x-rays than any other source and allow exposure times that are drastically shorter than those obtained with conventional sources; furthermore, the radiation is highly collimated, which eliminates any loss of resolution by penumbral blurring. The combination of an electron storage ring as the x-ray source, an x-ray resist as the detector, and a scanning electron microscope for viewing the resist profile therefore promises to provide a powerful technique for the study of biological objects.

In this report, we present some new results obtained with this technique. As x-ray sources we used both a source of carbon K$\alpha$ radiation [wavelength ($\lambda$) = 44.8 Å] and the radiation of the DESY (Deutsches Elektronen-Synchrotron) accelerator in Hamburg. Shorter exposure times are obtained with carbon K$\alpha$ than with the previously used aluminum K$\alpha$ radiation ($\lambda$ = 8.3 Å) (*2–5, 8*), because carbon K$\alpha$ radiation can be generated with high efficiency (*9*) and because the absorption of most resists increases with wavelength in the x-ray range.

For all experiments with the carbon source a 2.5-$\mu$m-thick film of Hostaphan (*10*) was used to support the objects and was mounted in front of the resist film in such a way that the objects faced the resist film. This made it possible to inspect both the original objects and their x-ray copy in the resist with a scanning electron microscope.

In the synchrotron experiments the objects were positioned directly on the resist surface before exposure and were washed off before development. The DESY synchrotron was operating at an energy of 3.5 Gev and the synchrotron radiation was reflected from a gold mirror at a glancing angle of 4° (*11*) in order to eliminate the hard radiation, which gives very little contrast.

Some of our results are shown in Fig. 2. Figure 2a is an x-ray micrograph of a diatom obtained with carbon radiation and Fig. 2b is a scanning electron micrograph of the same object. The x-ray micrographs in Fig. 2, c and d, were obtained with synchrotron radiation. The photographs show that features with dimensions around 1000 Å have enough absorption to give good contrast in the x-ray copy. Figure 2, a and b, demonstrates that the x-ray micrograph can detect the interior structure of an object, while the scanning electron microscope shows the surface structure. The curve showing the dissolution rate of the resist as a function of exposure is known and can be used to estimate the absorption in different parts of the specimen. We expect that replicas obtained with different wavelengths can reveal different structures in the object, depending on the composition of these structures. All our micrographs were obtained with the specimen in a vacuum. However, only minor modifications of our exposure station are necessary to allow exposure in air or helium, so that wet samples may be observed.

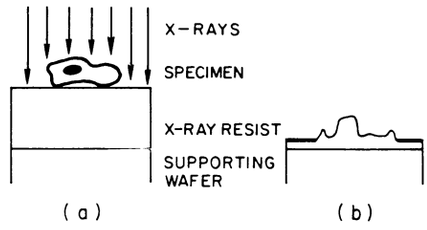


Fig. 1. (a) Irradiation of the x-ray resist through the specimen. In x-ray lithography the specimen is a mask generated by an electron beam. (b) The replica after development of the resist. The replica can be metallized and examined in a scanning electron microscope. In x-ray lithography the resist is completely removed in the fully exposed area, opening up this area for subsequent device fabrication steps.

The biggest advantage of synchrotron radiation for x-ray micrography is the drastically reduced exposure time. Exposure times on the order of seconds can be expected with storage rings such as DORIS (Doppel-Ring-Speicher) in Hamburg or with dedicated storage rings especially designed as sources of synchrotron radiation (*12*). With such dedicated sources the effective wavelength can be readily changed by changing the energy of the electrons in the storage ring.

With the combination of a dedicated storage ring, an x-ray resist, and a scanning electron microscope it should be pos-

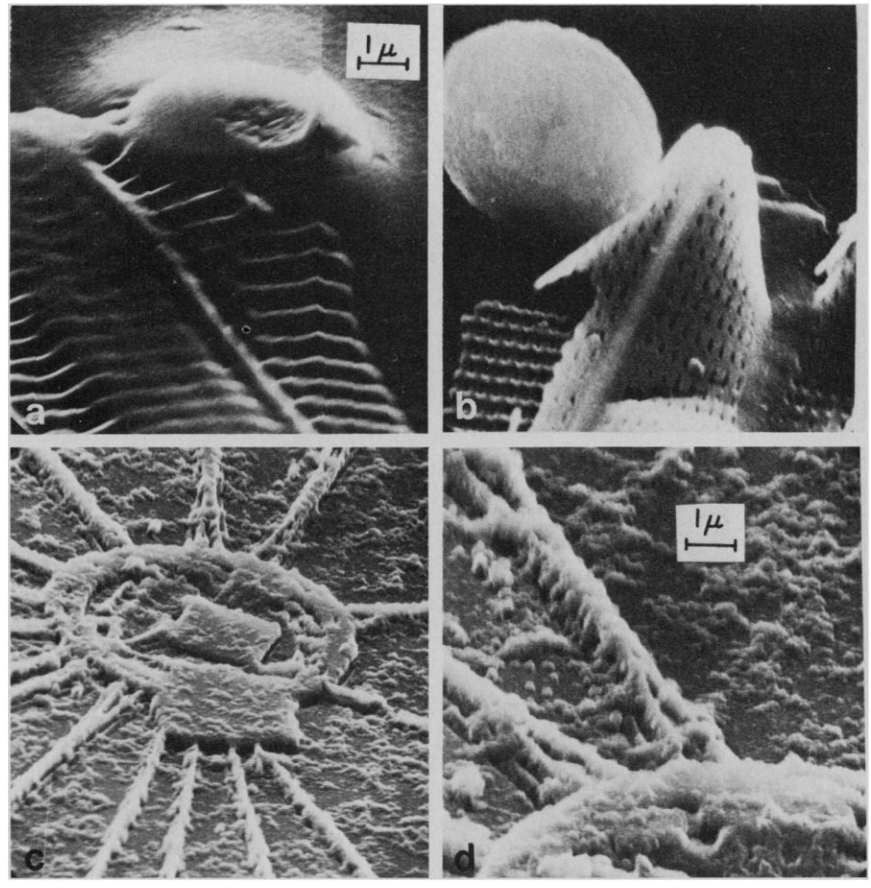


Fig. 2. X-ray replicas of diatoms (a, c, and d) in x-ray resist obtained with carbon radiation (a) and with synchrotron radiation (c and d). (b) Scanning electron micrograph of the object in (a), metallized with aluminum after the x-ray exposure. (d) Detail of (c). The x-ray exposure time was 20 hours with a source-to-specimen distance of 15 cm for (a) and 10 minutes with a distance of 40 m from the electron orbit of the synchrotron for (c) and (d). The x-ray resist was poly(methyl methacrylate).

sible to investigate biological specimens with resolutions near 100 Å. Improvements in x-ray resists should eventually make exposure times much shorter than 1 second possible.

E. SPILLER, R. FEDER
J. TOPALIAN, D. EASTMAN
W. GUDAT, D. SAYRE
*IBM Thomas J. Watson Research Center, Yorktown Heights, New York 10598*

### References and Notes

1. O. C. Wells, *Scanning Electron Microscopy* (McGraw-Hill, New York, 1974).
2. D. L. Spears and H. Z. Smith, *Electron. Lett.* **8**, 102 (1972).
3. R. Feder, E. Spiller, J. Topalian, *J. Vac. Sci. Technol.* **12**, 1332 (1975).
4. E. Spiller, R. Feder, J. Topalian, E. Castellani, L. Romankiw, M. Heritage, *Solid State Technol.*, in press.
5. H. H. Pattee, in *X-Ray Microscopy and X-Ray Microanalysis*, A. Engstrom, V. Cosslett, H. Pattee, Eds. (Elsevier, Amsterdam, 1960), p. 60; S. K. Asunmaa, in *X-Ray Optics and X-Ray Microanalysis*, H. H. Pattee, V. E. Cosslett, A. Engstrom, Eds. (Academic Press, New York, 1963), p. 33.
6. P. Horowitz and J. A. Howell, *Science* **178**, 608 (1972).
7. M. L. Perlonen, E. M. Rowe, R. E. Watson, *Phys. Today* **27**, 30 (July 1974).
8. R. Feder, D. Sayre, E. Spiller, J. Topalian, J. Kirz, *J. Appl. Phys.*, in press.
9. R. M. Dolby, *Br. J. Appl. Phys.* **11**, 64 (1960).
10. We thank Mr. Lopper of Kalle, Wiesbaden-Biebrich, Germany, for the Hostaphan samples.
11. H. J. Hagemann, W. Gudat, C. Kunz, *J. Opt. Soc. Am.* **65**, 742 (1975).
12. C. Kunz, in *Vacuum Ultraviolet Radiation Physics, Proceedings of the 4th International Conference, Hamburg, July 1974*, E. E. Koch, R. Haensel, C. Kunz, Eds. (Pergamon, Vieweg, 1974), pp. 753–771.
13. We thank Drs. C. Kunz and E. Koch and the staff of the radiation laboratory at Deutsches Elektronen-Synchrotron for their hospitality and support; Drs. D. Gould, B. Panessa, J. Studebaker, and S. Weaver for providing specimens; and Drs. J. Cocke, J. Kirz, and D. M. Kim for stimulating discussions.

23 October 1975; revised 9 December 1975

## Microwave Measurement of Mesospheric Carbon Monoxide

Abstract. *Ground-based observation of atmospheric absorption of solar radiation at a wavelength of 2.6 millimeters has provided the first measurement of mesospheric carbon monoxide. The measurement agrees with photochemical predictions of a carbon monoxide source in the lower thermosphere due to dissociation of carbon dioxide by solar radiation, and has implications for the magnitude of vertical transport in the mesosphere.*

Photochemical calculations predict that CO is produced in the earth's upper atmosphere by the solar ultraviolet dissociation of $CO_2$ (*1, 2*). We here report detection of the $J = 0 \rightarrow 1$ CO rotational transition at a frequency of 115,271.2 Mhz (wavelength, 2.6 mm) in the solar absorption spectrum. This absorption feature is due to CO in the earth's mesosphere and lower thermosphere and is the first experimental confirmation of the photochemical predictions. It provides a value for the CO column density at altitudes above $\sim 65$ km and information on the CO distribution in the altitude region $\sim 40$ to 80 km.

Ground-based microwave radiometric techniques like that used here for studying the earth's upper atmosphere were first suggested by Barrett and Chung (*3*), and are discussed in detail elsewhere (*4*). These techniques have previously been used to measure absorption or emission from ozone and molecular oxygen in the stratosphere (*5*). Voronov *et al.* (*6*) have also reported detection of the 115-Ghz CO line in the solar absorption spectrum. We are, however, suspicious of the measurement of Voronov *et al.*, since our analysis indicates that it implies a CO mixing ratio in the middle stratosphere which is $\sim 10^4$ times larger than that given by other measurements (*7*).

Our measurements were made on several days in April and May 1975 with the 4.6-m-diameter millimeter wavelength antenna and receiver of the Aerospace Corporation in El Segundo, California (latitude 34°N, sea level elevation). Measurements for 1 day are shown in Fig. 1. Although our data have not been closely examined for variations in the CO signal during the several days of measurement, no noticeable variation was apparent from a cursory examination. The beam width of the antenna was $\sim 0.1$ solar diameter; the spectral resolution of the multichannel filter bank used with the receiver was 0.25 Mhz and covered a total bandwidth of 8 Mhz. The frequency of the observed absorption line agrees exactly with laboratory measurements (*8*) of the $0 \rightarrow 1$ transition frequency of CO, proving that the line is due to CO, and the observed elevation dependence shows that it originated in the terrestrial atmosphere. The pressure-broadened half-width of the CO line in the atmosphere is $\sim 3$ Mhz/mbar, as discussed below, and the observed half-width of $\sim 0.3$ Mhz shows that the absorption occurred at pressures lower than $\sim 0.1$ mbar, corresponding to altitudes above $\sim 65$ km.

The absolute scale for the CO opacity $\Delta\tau_{CO}$ shown in Fig. 1 was determined from the expression

$$\Delta\tau_{CO} = \frac{\Delta T_A e^{m\tau}}{\eta_B T_\odot m} \quad (1)$$

where $\Delta T_A$ is the measured antenna temperature, calibrated by observation of sources whose temperatures are known; $T_\odot$ ($\sim 7000$°K) is the 2.6-mm brightness temperature of the sun, based on the data compiled by Linsky (*9*); $\eta_B$ is beam efficiency ($\sim 0.78$) calculated for the Aerospace antenna when observing the sun at 2.6 mm; $m$ is air mass; and $\tau$ is opacity at zenith of the lower atmosphere. (Thermal emission by the atmospheric CO adds another term in the denominator of Eq. 1, but this term is negligible.) The value of $\tau$ at the time of the measurement of Fig. 1 was determined to be 0.6 by observing the dependence of solar intensity with air mass. The difference in the values of $\tau$ corresponding to the two sidebands of our double-sideband receiver was approximately a factor of 2, based on our calculations and the data of Ulich and Haas (*10*), and was accounted for in determining $\tau$. We estimate the uncertainty in the absolute scale in Fig. 1 to be 10 percent.

The column density of CO above $\sim 65$ km can be deduced from the measured absorption feature. The absorption coefficient $k_\nu$ of this CO transition, within the range of atmospheric temperatures and frequencies $\nu$ sensed in our measurement, is

$$k_\nu = 7.4 \times 10^{-9} \frac{N_{CO}}{T^2} f(\nu)\ \text{cm}^{-1} \quad (2)$$

which can be obtained from standard absorption coefficient expressions and the known CO molecular parameters [for example, see (*11*)]. In Eq. 2 $N_{CO}$ is the CO number density in molecules per cubic centimeter, $T$ is temperature in °K, and $f(\nu)$ is the line shape function in seconds, normalized such that $\int f(\nu)d\nu = 1$. Integration of Eq. 2 over frequency and the observation path yields for the CO column density

$$\int N_{CO} dl = 1.4 \times 10^8 \langle T^2 \rangle \int \tau_\nu d\nu \quad (3)$$

where $\int N_{CO} dl$ is in molecules per square centimeter, $\langle T^2 \rangle$ is the average squared temperature of the absorbing CO molecules, $\tau_\nu = \int k_\nu dl$ is the opacity at frequency $\nu$, and $\int \tau_\nu d\nu$ is in reciprocal seconds. The measured value of $\int \tau_\nu d\nu$ corresponding to a zenith observation is $(1.8 \pm 0.2) \times 10^3$ sec$^{-1}$, which yields for the CO vertical column density above $\sim 65$ km

$$\int_{h > 65\ \text{km}} N_{CO} dh = (1.0 \pm 0.3) \times 10^{16}\ \text{cm}^{-2}$$

where $h$ is altitude. The uncertainty in the CO column density is due to the $\sim 10$ percent uncertainty in measurement accuracy and to the uncertainty in the temperature of the absorbing CO, which was assumed to be 200° ± 25°K, based on rocketsonde temperature data up to 70 km in altitude (obtained from the Point Mugu rocketsonde station 50 km northwest of the measurement location) and on model atmospheres above 70 km.

The shape of the absorption line provides information on the vertical distribution of CO. Below $\sim 75$ km collisional line